Numerical simulation and control of a continuous flow glass melting process using microwave radiation

Gonçalo Resende Moreira Feio
goncalo.feio@tecnico.ulisboa.pt

Instituto Superior Técnico, Universidade de Lisboa, Portugal

November 2020

Abstract

The industry of glass production plays an important role in the global energy consumption with significant CO_2 direct emissions to the atmosphere due to the conventional fossil fuels that are used as energy sources. In the past couple of decades considerable research has been made to switch the current energy sources to achieve reductions in the emissions of greenhouse gases. Among the alternatives, microwave radiation appears to be a promising one, with substantial advantages over the conventional heating sources.

This work aims to give insight on the microwave absorption heating mechanisms that take place in the continuous flow glass melting process. The commercial software *COMSOL Multiphysics* was used to solve the three-dimensional transient simulations with the coupling of the electromagnetic and thermal physics. A *MATLAB* algorithm was developed to autonomously control the process by adjusting the power input, required to achieve a specific output condition, and the microwave cavity geometry, to maximize the microwave efficiency. Several studies were performed with the objective of showing how different parameters influence the continuous glass melting process heated by microwave energy.

The developed *MATLAB* controller has proven to be a success, providing steady-state solutions for different operational conditions while respecting the requested output ones and using the minimum possible power. An innovative parametric study was conducted, and it allowed to find the operational conditions that maximize the global efficiency of the process. For these conditions, energy savings of almost 54% relatively to the conventional process were achieved.

Keywords: Microwave numerical modeling, High temperature microwave heating, Continuous flow microwave process, Autonomous microwave and thermal efficiency optimization, Microwave cavity design.

1. Introduction

The glass production industry plays an important role in the Europe's energy consumption, as well as in its CO_2 emissions, due to the high temperatures needed in the process of glass melting [1]. In order to reduce costs and emissions of greenhouse gases, major efforts have been made to improve the efficiency of the process of glass melting. Although this research is far from being complete, new energy sources are being extensively studied to reduce emissions and costs. In the last couple of decades, microwave energy started being used in glass processing with promising results namely in the quality of the final product and in time and energy savings [2,3].

Microwave heating is a very complex phenomenon which involves the two-way coupling of the Maxwell's and heat transfer equations due to the materials dielectric properties dependence on temperature [4]. Essentially, when a time-varying electric field reaches a dielectric medium, it suffers some attenuation and lagging mainly due to the polarization of dipolar molecules. This alternating reorientation of the molecules generates heat, result of friction mechanisms. The material response to the external electric field is measured by its complex permittivity, ϵ. There are several factors that influence microwave heating such as the physical properties of the material being heated, its geometry and location within the electric field, the frequency and operating mode of the external electric field, the geometry of the microwave cavity, etc. [5]. One of the most relevant parameters of microwave heating is the penetration depth, δ [m], which is the depth within the material where the external electric field amplitude falls to $1/e$ of its value at the material surface. The penetration depth decreases with the increase of the frequency of the electric field and with the increase of the loss factor, which is the imaginary part of the relative complex permittivity [6].

Concerning the environmental impact, microwave heating is preferable to the conventional one since it has no direct CO_2 emissions [7]. On the other hand, there are several physical mechanisms in microwave heating that can turn out to be disadvantageous. Firstly, since the electromagnetic field is strongly coupled with the thermal field it is necessary to establish a method to control the process in order to have efficiencies as high as possible, *i.e.*, by keeping the electric field peaks over the material to be heated. This can be done by changing the cavity geometry or the material position within the cavity. Secondly, some materials like glass and other ceramics, have a loss factor, *i.e.,* the imaginary part of the complex permittivity, that increases sharply with the temperature. Since the power absorbed by the material is proportional to the loss factor, a feedback mechanism usually called *thermal runaway* can occur leading to hotspots whose temperature grows uncontrollably [8-10].

Besides food industry where microwave heating has proven to be extremely effective, there are several other applications, namely in the glass industry, where this heating source is emerging with promising results.

Clemens and Saltiel [11] presented a detailed numerical model to solve the coupled electromagnetic-thermal problem using the finite difference time domain method (FDTD). The purpose of the study was to understand the influence of the working frequency, load size and dielectric properties of the heated material. Simulations with different load sizes indicated that there is a critical size which is related to the cut-off frequency phenomenon, *i.e.*, when the distance between the load and the cavity walls is less than half of a wavelength. The waves are strongly attenuated as they try to pass around the load and, consequently, the effective surface area for wave penetration is reduced leading to a power absorption decrease. Taking that phenomenon into account, the study reports that above the critical size, the microwave efficiency, *i.e.*, the ratio between the power absorbed and the power input, decreases. Below the critical size, the microwave efficiency rises until critical conditions are achieved.

Mimoso *et al.* [12] developed a numerical model in *COMSOL Multiphysics* in order to simulate the continuous microwave glass melting process in a single-mode cavity operating at $2.45\ \mathrm{GHz}$ in a TE_{10} mode with an alumina vertical container tube passing through it. A moving plunger was considered to allow the impedance matching during the simulations. In order to obtain steady-state solutions for different operation conditions with high microwave efficiency and sufficiently high outlet temperatures, a *MATLAB* code was developed to allow for both power input and plunger position control during successive transient electromagnetic-thermal simulations. The results obtained showed that the plunger adjustment has a significant impact on the steady-state microwave efficiency.

Yousefi *et al.* [13] developed a numerical model on *ANSYS Multiphysics* software to investigate the effects of inlet velocity, cavity height and applicator tube diameter on the process of microwave heating of continuous flowing water. Regarding the effect of the inlet velocity, the results showed that the power absorbed increased with the inlet velocity. Since the power input was kept constant, it implies that a rise in the inlet velocity will cause an increase in the microwave efficiency. This was justified by the increase of the water dielectric properties with decreasing temperature. As for the influence of the applicator tube diameter, the results showed that there is a critical diameter that is dependent on the dielectric properties, which decreases with the increase of the loss tangent. This agrees with the conclusions drawn by Clemens and Saltiel [11]. For diameters below the critical value, the microwave efficiency increases with increasing inlet velocity as discussed above. However, the results showed that for diameters above the critical value, the microwave efficiency decreases with increasing inlet velocity.

The main objective of this work is to develop a numerical model to study the continuous flow glass melting process, while using microwave radiation as the heating source. *COMSOL Multiphysics* is the selected commercial software since it has been widely used in several studies involving the coupling of electromagnetic and heat transfer physics [10],[12]. In order to obtain steady state solutions with maximum efficiency, minimized power input and with all the material to be processed at the outlet, a *MATLAB* algorithm will be developed following the previous works of Mimoso *et al.* [12] and Mendes [14]. It is the purpose of this work to analyze the evolution of the glass heating and melting process. A parametric study will be carried out to study the influence of the applicator tube inner diameter and mean flow velocity in the global efficiency of the process.

2. Background

2.1. Maxwell's equations

The Maxwell's equations are a set of four equations that constitute the basis for the electromagnetic theory, describing the interaction between the electric and magnetic fields. Faraday's law of induction, Maxwell-Ampere's law, electric and magnetic Gauss's laws are, respectively, found below:

$$\nabla \times \vec{E} = -\frac{\partial \vec{B}}{\partial t} \tag{1}$$

$$\nabla \times \vec{H} = \vec{J} + \frac{\partial \vec{D}}{\partial t} \tag{2}$$

$$\nabla \cdot \vec{D} = \rho_q \tag{3}$$

$$\nabla \cdot \vec{B} = 0 \tag{4}$$

where $\vec{E}$ is the electric field $[\mathrm{V/m}]$, $\vec{B}$ is the magnetic flux density $[\mathrm{Wb/m^2}]$, $\vec{H}$ is the magnetic field $[\mathrm{A/m}]$, $\vec{J}$ is the

electric current density [$\mathrm{A/m^2}$], $\vec{D}$ is the electric displacement or electric flux density [$\mathrm{C/m^2}$], ρ_q is the charge density [$\mathrm{C/m^3}$] and t is time [s]. The following equations are the constitutive relations that describe the macroscopic properties of a linear isotropic medium, where the electric and magnetic fields exist, and show how those fields relate to each other:

$$\vec{D} = \epsilon\vec{E} \tag{5}$$

$$\vec{B} = \mu\vec{H} \tag{6}$$

$$\vec{J} = \sigma\vec{E} \tag{7}$$

where ϵ is the permittivity [$\mathrm{F/m}$], μ is the permeability [$\mathrm{H/m}$] and σ is the electrical conductivity [$\mathrm{S/m}$] of the medium. Assuming that the fields have an harmonic time dependence, phasor notation can be applied and Equations (1) and (2) can be rewritten as:

$$\nabla \times \vec{E} = -j\omega\vec{B} \tag{8}$$

$$\nabla \times \vec{H} = \vec{J} + j\omega\vec{D} \tag{9}$$

2.2. Complex permittivity and penetration depth

Assuming that all the fields are time-harmonic, recalling Equation (5) and knowing that:

$$\vec{D} = \epsilon\vec{E} = \epsilon_0\vec{E} + \vec{P} \tag{10}$$

where ϵ_0 is the permittivity in vacuum and $\vec{P}$ is the polarization [$\mathrm{C/m^2}$], the vector $\vec{D}$ is the result of the sum of two harmonic waves. Due to polarization of dipole molecules there is a lag in phase between $\vec{P}$ and $\vec{E}$. Knowing that the sum of harmonic waves with the same angular frequency, ω, but with different phase angles, is still an harmonic wave with the same angular frequency, ω, but with different phase angle, it can concluded that $\vec{D}$ will not be in phase with $\vec{E}$. This means that the permittivity, ϵ, must be a complex number:

$$\epsilon = |\epsilon|e^{-j\delta_t} = \epsilon' - j\epsilon'' = \epsilon_0(\epsilon_r' - j\epsilon_r'') \tag{11}$$

where ϵ_r' is the real part of the relative permittivity, usually known as dielectric constant, ϵ_r'' is the imaginary part of the relative permittivity, known as loss factor and $\delta_t = \tan^{-1}(\epsilon_r''/\epsilon_r')$ is the phase mismatch between $\vec{D}$ and $\vec{E}$. In the literature $\tan\delta_t$ is known as the loss tangent and its value gives information about the material ability to absorb microwave radiation and converting it into heat [15]. The dielectric constant, ϵ_r', describes the ability of the material to store electric energy.

The penetration depth, δ [m], is an extremely important parameter in microwave heating. By definition δ is the depth within the material where the external electric field amplitude has dropped to $1/e$, around 37%, of its value at the material surface. The value of the penetration depth is given by [6]:

$$\delta = \frac{c}{2\pi f(2\epsilon_r')^{1/2}}\left\{\left[1 + \left(\frac{\epsilon_r''}{\epsilon_r'}\right)^2\right]^{1/2} - 1\right\}^{-1/2} \tag{12}$$

where $c = 1/\sqrt{\mu_0\epsilon_0}$ is the speed of light in vacuum [$\mathrm{m/s}$] and μ_0 is the permittivity in vacuum. Regarding Equation (12) it can be concluded that the penetration depth is influenced by the working frequency, f, decreasing as the frequency increases. It is also dependent on the dielectric constant, ϵ_r', and on the loss tangent, ϵ_r''/ϵ_r', decreasing as both parameters increase.

2.3. Poynting Theorem and microwave dissipated power

The cross product between the electric and magnetic fields is called the Poynting vector, $\vec{S}$, and has units of $\mathrm{W/m^2}$, which means that it represents an energy flux density. For a closed surface S, the energy flux that crosses it is given by:

$$\oiint_S (\vec{E}\times\vec{H})\cdot\vec{n}\,dS = \iiint_{V_s}\left[-\vec{H}\cdot\frac{\partial\vec{B}}{\partial t} - \vec{E}\cdot\frac{\partial\vec{D}}{\partial t} - \vec{J}\cdot\vec{E}\right]dV \tag{13}$$

Equation (13), which consists in an electromagnetic energy balance, expresses the Poynting theorem. It states that the amount of power that leaves the enclosed surface, S, equals the rate of decrease of stored electric and magnetic energies plus the losses that are dissipated within the volume, V_s. If it is assumed that all the fields are time-harmonic, the so-called complex phasor form of the Poynting theorem can be written as:

$$\begin{aligned}\oiint_S (\vec{E}_s\times\vec{H}_s^*)\cdot\vec{n}\,dS = -j\omega\iiint_{V_s}(\mu_0 H_0^2 - \epsilon_0\epsilon_r' H_0^2)\,dV \\ - \iiint_{V_s}(\sigma + \omega\epsilon_0\epsilon_r'')E_0^2 dV\end{aligned} \tag{14}$$

It can be shown that the real part of Equation (14) represents twice the time-averaged power that crosses the closed surface S. The expression:

$$Q = (\sigma + \omega\epsilon_0\epsilon_r'')\,E_0^2/2 \tag{15}$$

which units are $\mathrm{W/m^3}$, represents the power that is dissipated and converted into heat by Joule effect and mainly by friction mechanisms due to the dipolar relaxation phenomena.

2.4. Momentum and continuity equations

A laminar, incompressible flow is characterized by the continuity and Navier-Stokes equations, respectively:

$$\nabla\cdot\vec{U} = 0\,; \qquad \frac{\partial\vec{U}}{\partial t} + \vec{U}\cdot\nabla\vec{U} = -\frac{\nabla P}{\rho} + \nu\nabla^2\vec{U} \tag{16}$$

where $\vec{U}$ is the velocity [$\mathrm{m/s}$], P is the pressure [Pa], ρ is the fluid density [$\mathrm{kg/m^3}$] and ν is the kinematic viscosity [$\mathrm{m^2/s}$]. The continuity equation, which describes a mass balance, shows that for an incompressible fluid, *i.e.*, when ρ is contant, the divergence of the velocity is zero. The

Navier-Stokes equation represents a momentum balance for an infinitesimal control volume.

2.5. Heat equation

The non-stationary heat transfer process is described by the transient heat equation which gives the thermal field solution:

$$\frac{\partial}{\partial t}\left(\rho C_p T\right) + \vec{U}\cdot\nabla\left(\rho C_p T\right) = \nabla\cdot(k\nabla T) + Q \qquad (17)$$

where C_p is the specific heat capacity $[\mathrm{J/(kg\cdot K)}]$, T is the temperature [K], k is the thermal conductivity $[\mathrm{W/(m\cdot K)}]$ and Q $[\mathrm{W/m^3}]$ is the heat source term. The second term on the right-hand side, Q, is the power source which enables the coupling of the Maxwell's equations with the heat transfer one. Regarding Equation (15), it is important to observe that two heating mechanisms are present, which are the Joule and the dielectric loss effects, represented, respectively, by the following expressions:

$$Q_J = \sigma\frac{E_0^2}{2}\,; \qquad Q_D = \omega\epsilon_0\epsilon_r''\frac{E_0^2}{2} \qquad (18)$$

2.6. Numerical simulations with *COMSOL Multiphysics*

It was previously stated that the process of microwave heating involves the coupling of the Maxwell's and heat equations. Since the thermal and dielectric properties of glass are highly dependent on temperature, an iterative method is necessary to obtain a coupled solution. If it is assumed that the electromagnetic fields are harmonic and the frequency is fixed, some simplifications can be made in the Maxwell's equations, and after some algebra the Helmholtz equation in the frequency domain is obtained:

$$\nabla\times\frac{1}{\mu_r}\left(\nabla\times\vec{E}\right) - k_0^2\epsilon_r'\vec{E} + jk_0^2\left(\frac{\sigma}{\omega\epsilon_0} + \epsilon_r''\right)\vec{E} = 0 \qquad (19)$$

Given an initial temperature distribution, the electric field is calculated using Equation (19). The microwave power dissipated is then calculated using Equation (15) and introduced in the heat equation. After that, the thermal field is computed using Equation (17) and the temperature dependent properties are updated, before the Helmholtz equation is solved again. This iterative scheme is repeated until a solution is achieved.

3. Numerical model

3.1. Geometry and material properties

In order to numerically simulate the glass melting process, a geometry of the microwave cavity was defined, which consists of a standard WR-340 rectangular waveguide behaving as a single-mode cavity vertically trespassed by an applicator tube, where the glass flows. The exterior walls of the cavity and tube are covered by an insulation material intended to minimize the thermal losses. For a better visualization, the geometry described above is depicted in Figure 1. The microwave cavity is filled with air and its length is controlled by the plunger position. In order to keep the electric field peak near the load location, maximizing the microwave efficiency, the plunger position varies during the heating process.

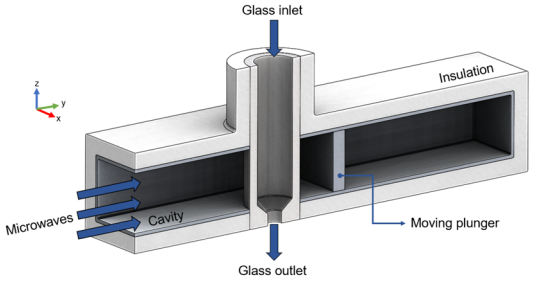

Figure 1: Microwave cavity geometry designed for the numerical study of the glass melting process.

Regarding the materials used in each domain, an aluminum alloy was chosen for the cavity walls and moving plunger and an alkaline earth silicate wool was considered for the insulation. Boron nitride was the selected material for the applicator tube due to its high operating temperature and microwave transparency behavior and a soda-lime silica glass was the material chosen to be processed and studied in this work. Data for the glass density, $\rho(T)$, dielectric constant, $\epsilon_r'(T)$, and loss factor, $\epsilon_r''(T)$, were provided by [16]. To obtain the temperature dependent curves of the thermal conductivity, $k(T)$, and specific heat capacity, $C_p(T)$, a mass weighted method was applied considering the data found in the literature. Information about the thermal conductivity was found in [17-19]. As for the specific heat capacity, information was obtained in [20]. A reference value for the emissivity of glass powder, ε, and for the glass melting temperature, T_m [K], was found in [21-22], respectively. Concerning the value of the latent heat of fusion, L_f $[\mathrm{J/kg}]$, a mass weighted value was obtained with the information found in [20]. Data for the dynamic viscosity, μ_v $[\mathrm{Pa\cdot s}]$, was obtained in [23]. During the numerical simulations, a linear extrapolation was used for temperatures outside of the ranges, which were defined by the data available in the literature.

3.2. Boundary and initial conditions

All the boundaries of the wave equation domain were considered as *perfect electric conductor*, except for the cavity inlet and tube inlet and outlet boundaries, where *port* and *scattering* boundary conditions were used, respectively. In this study, the *port* boundary simulates the inlet of a $\mathrm{TE_{10}}$ wave with a specified power, P_{in} [W], at a 2.45 GHz fixed frequency. The *scattering* boundary condition simulates microwave leakage in the boundaries where it was applied.

Concerning the boundary conditions used in the thermal interface, an *outflow* boundary condition was given to the applicator tube outlet surface. Radiation and

natural convection heat fluxes were imposed to the exterior surfaces of the microwave cavity and the ambient temperature, T_{amb}, was set to 293 K. The convection coefficients, h, were calculated for all the exterior surfaces depending on their orientation relatively to the gravitational vector, $\vec{g}$, using empirical correlations found in [24-25]. To consider the energy exchange by radiation between the interior walls of the microwave cavity, the *diffuse surface* boundary condition was applied in those regions simulating surface-to-surface radiative heat fluxes.

Finally, at the applicator tube inlet, a *heat flux* boundary condition was applied, which represents the power required to rise the glass temperature from T_0 to T. This heat flux, integrated over the inlet area, S_{in}, is given by:

$$Q_{in} = \iint_{S_{in}} \left[\rho(\vec{U} \cdot \vec{n}) \int_{T_0}^{T} C_p(T) dT \right] dA \tag{20}$$

where $\vec{U}$ is the local velocity [m/s], $\vec{n}$ is the surface unit normal vector, T_0 is the temperature at which the glass is introduced in the system [K], defined as $T_0 = 293\ K$, and T is the local temperature [K]. As for the initial conditions, a temperature of 293 K was set to all domains except for the glass region, where a linear temperature profile was assigned, with a value of 293 K at the inlet and a value of 1293 K at the outlet.

With respect to the boundary conditions applied to the flow interface, the inner walls of the applicator tube were modelled with a *no-slip* boundary condition. For the inlet surface a *mass flow* boundary condition was applied and atmospheric pressure was imposed at the outlet surface.

3.3. Phase change numerical modelling

There are several methods to model numerically a material phase-change. *COMSOL* uses an apparent specific heat capacity, $C_{p_{app}}(T)$, in the heat equation to account for the glass phase-change and given by:

$$C_{p_{app}}(T) = C_p(T) + L_f \frac{d\theta}{dT} \tag{21}$$

where θ represents the fraction of liquid phase, modelled as a smooth ramp function in the temperature interval between $T_m - \Delta T/2$ and $T_m + \Delta T/2$, where ΔT is a user defined parameter that specifies the temperature difference between the beginning and the end of the phase change process.

3.4. *MATLAB* microwave melting controller code

To understand the controlling process developed in this work, some concepts must firstly be introduced to the reader. The fraction of the power input that is reflected is given by:

$$\frac{P_{ref}}{P_{in}} = |S_{11}|^2 \tag{22}$$

where P_{ref} [W] and P_{in} [W] are the reflected and input microwave powers, respectively, and S_{11} is the reflection coefficient. Since the model can compute the radiation leakage, P_L [W], that may occur across the tube inlet and outlet, the microwave efficiency, η_{MW}, is given by:

$$\frac{P_{abs}}{P_{in}} = \eta_{MW} = 1 - |S_{11}|^2 - \frac{P_L}{P_{in}} \tag{23}$$

where P_{abs} [W] is the microwave power absorbed by the glass and tube. The thermal efficiency, η_T, which is the fraction of the absorbed power that actually contributes to the heating and phase change of the glass, since some of it will be lost by radiation and convection across the external surfaces of the microwave cavity is given by:

$$\eta_T = \frac{P_h}{P_{abs}} \tag{24}$$

where P_h is the sum of the sensible heat, SH [W], responsible for the glass temperature rise from T_0 to T, which is the local temperature at the tube outlet, and the latent heat, LH [W], responsible for the glass phase change:

The global efficiency of the process, η_G, represents the fraction of the total power input that contributes to the melting of the glass, and is given by:

$$\eta_G = \frac{P_h}{P_{in}} \theta = \eta_{MW} \eta_T \theta \tag{25}$$

where the variable θ is used to penalize the global efficiency when the glass is not totally processed when leaving the system.

The main goal of this work is to simulate the glass melting process and study the influence of several operational conditions on its global efficiency, η_G. To achieve this objective, at steady-state, the glass must be totally in a melted state at the tube outlet, so it is necessary to provide enough microwave power to rise the glass temperature from T_0 to a temperature, T, which must be greater than the glass melting temperature, T_m. Since $T_m = 1450$ K, it was decided that an outlet average temperature of $T_{out} = 1600$ K should be obtained at steady-state. Besides the required sensible heat, the latent heat must be considered, *i.e.*, the additional power for the phase-change. The latent heat is defined by the material's mass flow rate times its latent heat of fusion. Since the microwave cavity is not completely insulated, thermal losses, P_{loss} [W], will arise as the system temperature increases. To achieve the desired outlet average temperature, the power input must account for those thermal losses. To achieve the desired outlet conditions, another essential parameter that must be considered in the calculation of the power input is the microwave efficiency. The required microwave power input is given by:

$$P_{in} = \frac{\dot{m} \int_{T_0}^{T_{out}} C_p(T) dT + \dot{m} L_f + P_{loss}}{\eta_{MW}} \quad (26)$$

To get a converged solution with the desired outlet conditions using the required power input it is necessary to run transient simulations during a defined physical time, Δt_s. After each simulation, both microwave efficiency and thermal losses must be extracted from the results in order to update the power input. This process must be repeated until the transient term of the heat equation is below a user defined limit, meaning that steady-state was achieved. Being this is a very time-consuming method that requires constant supervision, a *MATLAB* code was developed to automatically control the glass melting process.

The *MATLAB* controller code consists of the following steps:

1. Set the input parameters for the *MATLAB* code, namely: the material mass flow rate, the tube's inner diameter, the desired glass outlet average temperature, $T_{out} = 1600\ \mathrm{K}$ in this Thesis, the glass inlet temperature, the physical duration of the transient simulations, the initial plunger position and the initial microwave efficiency.
2. With the data given in 1, compute the initial power input using Equation (26) assuming no thermal losses since they are not known *a priori*.
3. Load the *COMSOL* model.
4. Assign the data given in 1 and the power input computed in 2 to the *COMSOL* model.
5. **Start 1st loop**: Getting a steady-state solution.
   5.1. Run a transient simulation with a total time of Δt_s.
   5.2. Extract all the relevant data, namely the thermal losses, the microwave leakage, the value of the transient term of the heat equation and the power absorbed by the glass.
   5.3. **Start 2nd loop**: Plunger position update.
      5.3.1. Run a parametric study for the actual and adjacent plunger positions.
      5.3.2. If the maximum value of $1 - |S_{11}|^2$ is found on the actual position, with the microwave leakage obtained in 5.2 compute the new microwave efficiency. Leave 2nd loop and go to point 5.4.
      5.3.3. If not, the position with the highest value for $1 - |S_{11}|^2$ is defined as the actual one and start 2nd loop again from point 5.3.1.
   5.4. Compute the new power input with the data extracted in 5.2 and computed in 5.3.2 using Equation (26).
   5.5. If the value of the transient term of the heat equation is less than 0.1% of the power absorbed by the glass, steady-state solution has been achieved. Save the converged model. Leave 1st loop and go to point 6.
6. End of the *MATLAB* controller code.

4. Results and discussion

4.1. Melting process control and converged solution

This section presents the evolution of the melting process controlled by the *MATLAB* code until steady-state is achieved for a mass flow rate of $\dot{m} = 3.6\ \mathrm{kg/h}$ and tube inner diameter of $d_i = 30\ \mathrm{mm}$. To improve the heating uniformity, rotation was imposed to the tube. In the following figures, some relevant variables are plotted versus the physical time. In Figure 2.a, the evolution of the control variables from the *MATLAB* algorithm are presented. Regarding the microwave efficiency curve, it is observed that after the initial iterations, the plunger adjustment has little influence on the microwave efficiency. This behavior can be explained by the cut-off frequency phenomenon reported in [11,13,15].

As the temperature of the glass starts to increase, so do its dielectric properties [16]. Recalling Equation (12), the penetration depth, δ, decreases when the dielectric properties increase and, since, in the present case, the ratio δ/r_i is very small, being r_i the inner radius of the applicator tube, the microwave absorption occurs in a thin layer facing the incoming radiation, which sees the glass material as a poor absorber. So, for the present case where tube's inner diameter is $d_i = 30\ \mathrm{mm}$, the distance between the tube's inner surface and the waveguide walls is not enough to allow the propagation of the radiation, meaning that the electric flied is very low in the region between the load and the moving plunger. For that reason, the plunger position adjustment has little influence on the microwave efficiency in this configuration.

Regarding the power input evolution, it is observed that its continuous increase is mainly caused by the decrease in the microwave efficiency following Equation (26). The thermal losses across the exterior boundaries of the microwave cavity also contribute to the power input increase. Relatively to the plunger position adjustment, it has been mentioned that, for the present case, it has little influence on the microwave efficiency after the first couple of iterations. However, by running another simulation with $d_i = 15\ \mathrm{mm}$, keeping the same mean flow velocity, it was observed that the influence of the plunger position adjustments in the glass heating process is clearly dependent on the tube's inner diameter, d_i, increasing as the latter decreases, since for smaller diameters the cut-off frequency effect has a lower influence. These results showed that the use of plunger position adjustments is always a better solution than keeping the moving plunger in a fixed position, allowing a microwave efficiency increase of 2.5% and 12% for the cases with $d_i = 30\ \mathrm{mm}$ and $d_i = 15\ \mathrm{mm}$, respectively.

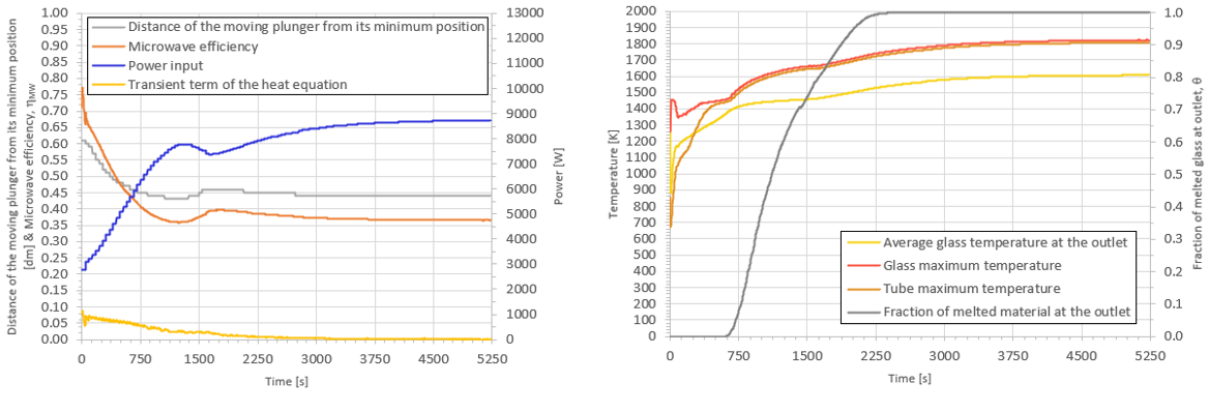

(a) (b)

Figure 2: (a) Power input, microwave efficiency, transient term of the heat equation and plunger position, (b) average outlet glass temperature, maximum glass temperature, maximum tube temperature and outlet fraction of melted material evolutions during the physical time.

With respect to the transient term of the heat equation, it is shown that it approaches zero from positive values, meaning that the energy of the system is increasing, resulting in the rise of the glass temperature, until steady-state is achieved.

Figure 2.b presents the evolution of the glass average outlet and maximum temperatures, the tube maximum temperature and the outlet fraction of melted glass. Regarding the glass average outlet temperature, it is noticed that during the first iteration, its value drops sharply. This happens because, in the first iteration, the *MATLAB* controller does not consider the thermal losses when computing the required power input. After the first iteration, the glass average outlet temperature continuously rises until it stabilizes at $1607\,\mathrm{K}$ when steady-state is achieved. It is also important to observe that, after the initial phase of the heating process, the tube maximum temperature approaches the glass maximum temperature, both being practically the same during the rest of the simulation. This happens because, as verified above, the microwave absorption occurs in a very thin layer of glass near the tube's inner walls, so both maximum temperature locations are near each other reducing the margin for differences. The curve representing the outlet fraction of melted glass shows that, at steady-state, the exiting glass is completely processed as desired. The overall steady-state results are summarized in Table 1 and show that the *MATLAB* controller can provide a steady-state solution with the required outlet conditions. The low global efficiency value is clearly related to the low ratio δ/r_i, which suggests that smaller diameters should be used.

4.2. Tube inner diameter and mean flow velocity combined parametric study

In this subsection a parametric study is presented to show how the tube inner diameter and mean flow velocity affect the global efficiency of the melting process and thus to give some support in the design stage of a microwave continuous system, and also to find the operational conditions that maximize the global efficiency of this process within the given study domain. To find the best operational conditions, several simulations were done with different values of d_i and U_{ave}. The analyzed tube inner diameters and mean flow velocities were changed in the intervals $12.5\,\mathrm{mm} \leq d_i \leq 30\,\mathrm{mm}$ and $0.64\,\mathrm{mm/s} \leq U_{ave} \leq 11.50\,\mathrm{mm/s}$, respectively.

Table 1: Steady-state results for the glass melting process with $d_i = 30\,\mathrm{mm}$ and $\dot{m} = 3.6\,\mathrm{kg/h}$.

Variable	Value
Power input, P_{in} [W]	8722
Sensible heat at outlet [W]	1553
Latent heat at outlet [W]	388
Thermal losses, P_{Loss} [W]	1251
Outlet Fraction of melted material, θ [%]	100
Glass average outlet temperature, T_{out} [K]	1607
Microwave efficiency, η_{MW} [%]	37
Thermal efficiency, η_T [%]	61
Global efficiency, η_G [%]	23

For each simulation, the converged values for the microwave efficiency, η_{MW}, thermal efficiency, η_T, outlet fraction of melted material, θ, and global efficiency, η_G, were stored and plotted against both d_i and U_{ave} creating three-dimensional surfaces. These surfaces are presented in Figure 3 in a top view for better visualization. The global efficiency surface provides the information about the combination between d_i and U_{ave} that should be used to minimize the energy consumption in the glass melting process. However, since the global efficiency is obtained from the product between the values of η_{MW}, η_T and θ, to understand its behavior, it is indispensable to firstly examine the trends of the other three quantities. In the first place, a detailed description of the microwave effi-

ciency surface will be given, followed by a briefer description of the η_T and θ ones.

By observing Figure 3.a, which represents the microwave efficiency dependence on both d_i and U_{ave}, it can be observed the existence of two classes of diameters. For the second-class diameters, $d_i \geq 20\ \text{mm}$, there is a clear tendency for the microwave efficiency to continuously decrease as the mean flow velocity increases. This happens due to the strong influence of the cut-off frequency effect and to the low penetration depths observed in the glass material, caused by the very high values of its dielectric properties at high temperatures [16]. For smaller diameters, belonging to the first class where $12.5\ \text{mm} < d_i < 20\ \text{mm}$, the microwave efficiency firstly increases with the mean flow velocity and at a certain critical point reaches a maximum value. Then, for velocities higher than the critical one, the microwave efficiency starts to drop. The evolution of this surface also shows that the microwave efficiency tends to continuously increase as the tube inner diameter decreases for all mean flow velocities studied. It is, however, important to recall that this tendency is strongly related to the lower penetration depths of the glass at high temperatures.

Figure 3.b, shows that for almost all simulations the glass leaves the tube totally processed. It is only for large diameters and with high mean flow velocities that the value of θ starts to drop and affects the global efficiency. Analyzing Figure 3.d, it can be stated that the thermal efficiency continuously grows with the increase of both d_i and U_{ave}. After analyzing the microwave and thermal efficiencies surfaces as well as the variation of the outlet fraction of melted material in the defined study domain, Figure 3.c, describing the global efficiency, can be commented. It can be observed that, for all studied diameters, the global efficiency rises with the increase of the mean flow velocity until a critical value is reached, where a maximum efficiency is achieved. In a general way, this critical velocity increases as the diameter decreases. After the critical velocity, the global efficiency tends to drop and then stabilize.

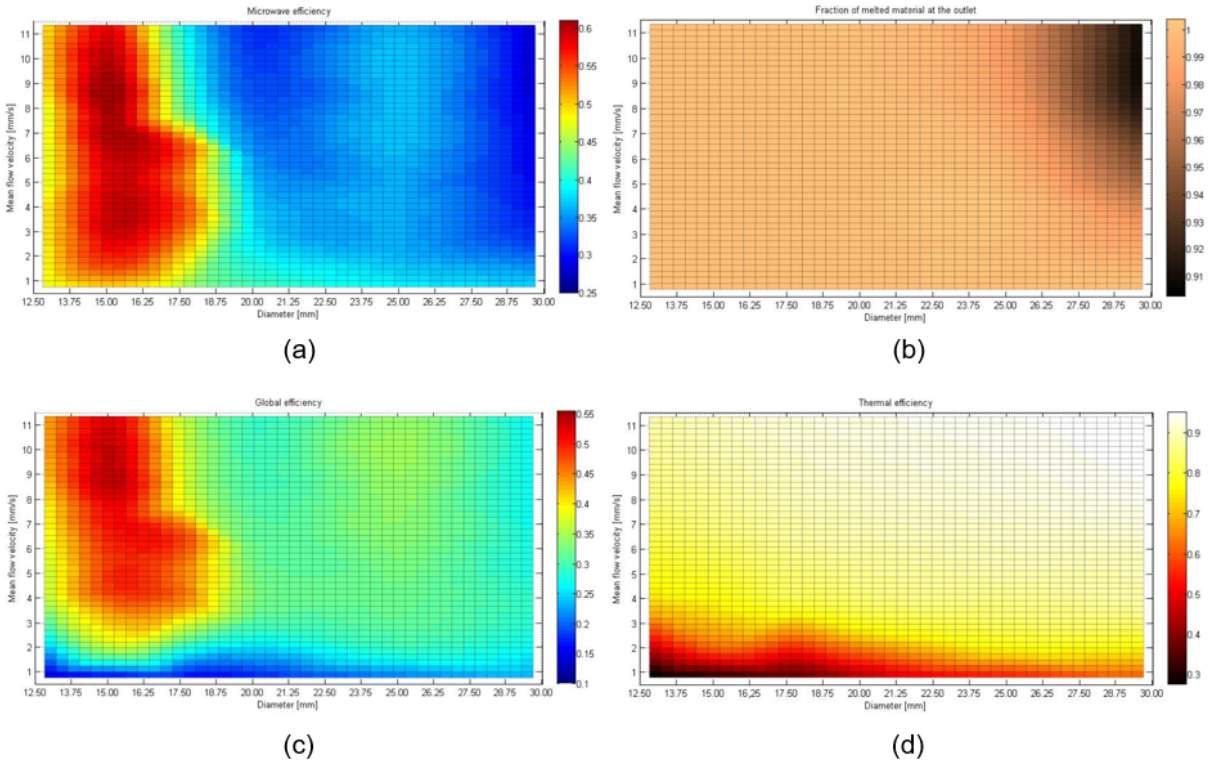

Figure 3: Combined influence of the tube inner diameter, d_i [mm], and mean flow velocity, U_{ave} [mm/s], on the (a) microwave efficiency, η_{MW}, (b) outlet fraction of melted material, θ, (c) global efficiency, η_G, and (d) thermal efficiency, η_T

This behavior is due to the influence of the thermal efficiency on the microwave process. For low velocities, the global efficiency curve shows low values due to the very low thermal efficiencies.

Since for high mean flow velocities, the thermal efficiency tends to stabilize for values close to unity, its influence on the global efficiency vanishes. On the other hand, the curve of θ only affects the global efficiency for diameters close to $d_i = 30\ \text{mm}$ at very high velocities. For that reason, and since the highest values of the microwave efficiency are in the region where the thermal efficiency has little influence and the value of θ has no

influence at all, the parameters that maximize the global efficiency are $d_i = 15\ \text{mm}$ and $U_{ave} = 8.50\ \text{mm/s}$, corresponding to a mass flow rate of $\dot{m} = 11.92\ \text{kg/h}$. The converged results for these operational conditions are summarized in Table 2 and illustrated in Figure 4.

Table 2: Steady-state results for the glass melting process with $d_i = 15\ \text{mm}$ and $\dot{m} = 11.92\ \text{kg/h}$.

Variable	Value
Power input, P_{in} [W]	11952
Power absorbed, P_{abs} [W]	7331
Sensible heat at outlet [W]	5129
Latent heat at outlet [W]	1286
Thermal losses, P_{Loss} [W]	916
Microwave efficiency, η_{MW} [%]	61
Thermal efficiency, η_T [%]	88
Global efficiency, η_G [%]	54
Specific energy consumption, SEC [kJ/kg]	3605

Observing the obtained value for the specific energy consumption, SEC, which represents the amount of energy required to process $1\ \text{kg}$ of glass, and comparing it to the reference value for the conventional process, $SEC_{conv} = 7800\ \text{kJ/kg}$ given in [1], it can be concluded that energy savings of almost 54% can be achieved using the microwave melting process.

The results showed that the microwave power reflected represents 24% of the microwave power input, while 15% is escaping as microwave leakage. For these operational conditions, a microwave efficiency of $\eta_{MW} = 61\%$ was achieved. Of the power that is effectively absorbed by both glass and tube, 70% is being used to heat the glass from $293\ \text{K}$ to $1600\ \text{K}$, 18% is being used in the glass phase change and only 12% is being lost as convection and radiation through the microwave cavity exterior walls. Since only the sensible and latent heat are useful power in the process, the thermal efficiency is, for this case, $\eta_T = 88\%$ and a global efficiency of $\eta_G = 54\%$ was achieved.

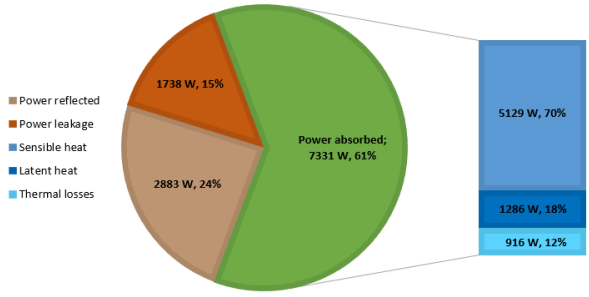

Figure 4: Complete energy balance of the microwave cavity for the case with $d_i = 15\ \text{mm}$ and $\dot{m} = 11.92\ \text{kg/h}$

5. Conclusions

A continuous flow microwave heating unit with the purpose of melting glass was developed and modelled in this work. The commercial software *COMSOL Multiphysics* was used to numerically simulate the glass melting process by coupling the electromagnetic and thermal physics. Three-dimensional transient simulations were run in order to achieve steady-state results with the desired outlet conditions and with the lowest possible power input. To reach this objective, the transient simulations were controlled by a developed *MATLAB* algorithm coupled to the *COMSOL* interface. This algorithm allowed to control the cavity geometry with a moving plunger, enabling the optimization of the process efficiency, and to control the power input delivered by considering the thermal losses, the microwave efficiency variations, as well as the power required to heat and melt the flowing material.

The thermal history for the given operational conditions was studied in detail showing that the *MATLAB* code was able to control the simulation until a steady-state solution was achieved. The results showed that the outlet conditions defined by the user were achieved and temperature-related problems, such as the *thermal runaway* phenomenon, were not observed.

The influence of the applicator tube inner diameter and mean flow velocity on the global efficiency of the glass melting process was analyzed through an innovative parametric study. The results showed that, for the defined study domain, operational conditions that maximize the global efficiency of the process can be found and that their values are strongly related to the penetration depth of the processed material which depends on its dielectric properties. For these conditions it was observed that using microwave energy as the heating source for melting glass allowed for energy savings of almost 54% relatively to the conventional process.

References

[1] A. Schmitz, J. Kamiński, B.M. Scalet and A. Soria. Energy consumption and CO_2 emissions of the European glass industry. *Energy Policy*, 39:142-155, 2011.

[2] D. Agrawal. Microwave sintering of ceramics, composites and metallic materials, and melting of glasses. *Transactions of the Indian Ceramic Society*. 65(3):129-144, 2006.

[3] A.K. Mandal, S. Sen, S. Mandal, C. Guha and R. Sen. Energy efficient melting of glass for nuclear waste immobilization using microwave radiation. *International Journal of Green Energy*, 12:1280-1287, 2015.

[4] Y. Alpert and E. Jerby. Coupled thermal-electromagnetic model for microwave heating of temperature-dependent dielectric media. *IEEE Transactions on Plasma Science*, 27(2):555-562, 1999.

[5] P.K. Loharkar, A. Ingle and S. Jhavar. Parametric review of microwave-based materials processing and its applications. *Journal of Materials Research and Technology*, 8(3):3306-3326, 2019.

[6] D. Nowak. The impact of microwave penetration depth on the process of heating the moulding sand with sodium silicate. *Archives of Foundary Engineering*, 17(4):115-118, 2017.

[7] C. Dorn, R. Behrend, D. Giannopoulos, L. Napolano, B. García Baños, V. James, V. Uhlig, J. M. Catalá, M. Founti and D. Trimis. KPI and LCA evaluation of integrated microwave technology for high temperature processes. *Procedia CIRP*, 29:492-497, 2015.

[8] C.A. Vriezinga, S. Sánchez-Pedreño and J. Grasman. Thermal runaway in microwave heating: a mathematical analysis. *Applied Mathematical Modelling*, 26:1029-1038, 2002.

[9] X. Wu, J.R. Thomas, Jr. and W.A. Davis. Control of thermal runaway in microwave resonant cavities. *Journal of Applied Physics*, 92(6):3374-3380, 2002.

[10] D. Salvi, D. Boldor, G.M. Aita and C.M. Sabliov. COMSOL Multiphysics model for continuous flow microwave heating of liquids. *Journal of Food Engineering*, 104:422-429, 2011.

[11] J. Clemens and C. Saltiel. Numerical modeling of materials processing in microwave furnaces. *International Journal of Heat and Mass Transfer*, 39(8):1665-1675, 1996.

[12] R.M.C. Mimoso, D.M.S. Albuquerque, J.M.C. Pereira and J.C.F. Pereira. Simulation and control of continuous glass melting by microwave heating in a single-mode cavity with energy efficiency optimization. *International Journal of Thermal Sciences*, 111:175-187, 2017.

[13] T. Yousefi, S.A. Mousavi, M.Z. Saghir and B. Farahbakhsh. An investigation on the microwave heating of flowing water: a numerical study. *International Journal of Thermal Sciences*, 71:118-127, 2013.

[14] J.P.M. Mendes. *Simulation of cement clinker process by of microwave heating*. Master thesis, Instituto Superior Técnico, Universidade de Lisboa, 2017.

[15] J. Zhu, A.V. Kuznetsov and K.P. Sandeep. Mathematical modeling of continuous flow microwave heating of liquids (effects of dielectric properties and design parameters). International Journal of Thermal Sciences, 46:328-241, 2007.

[16] http://microwavepropertiesnorth.ca/glasses_insulation_materials/ consulted on November 30th, 2019.

[17] S.C. Carniglia and G.L. Barna. *Handbook of industrial refractories technology. Principles, types, properties and applications*. Noyes Publications, 1992.

[18] E. Tatli, J.P. Mazzoccoli and P. Ferroni. CFD modeling of sodium-oxide deposition in sodium-cooled fast reactor compact heat exchangers. In *16th International Topical Meeting on Nuclear Reactor Thermalhydraulics Conference*, 2015.

[19] P. Auerkari. Mechanical and physical properties of engineering alumina ceramics. *VTT Tiedotteita*, 1792, 26, 1996.

[20] D.W. Green and R.H. Perry. *Perry's Chemical engineers' handbook*. McGraw-Hill, 8th edition, 2008.

[21] F. Albouchi, M. Fetoui, F. Rigollet, M. Sassi and S.B. Nasrallah. Optimal design and measurement of the effective thermal conductivity of a powder using a crenel heating excitation. *International Journal of Thermal Sciences*, 44:1090-1097, 2005.

[22] L. Pilon, G. Zhao and R. Viskanta. Three-dimensional flow and thermal structures in glass melting furnaces. Part 1. Effects of the heat flux distribution. *Glass Science and Technology*, 75(2):55-68, 2006.

[23] A. Napolitano and E.G. Hawkins. Viscosity of a standard soda-lime-silica glass. *Journal of Research of the National Bureau of Standards – A. Physics and Chemistry*, 68A(5):439-448, 1964.

[24] T.L. Bergman, A.S. Lavine, F.P. Incropera and D.P. Dewitt. *Fundamentals of heat and mass transfer*. John Wiley & Sons, 7th edition, 2011.

[25] G.D. Raithby and K.G.T. Hollands. Natural convection. In W.M. Rohsenow, J.P. Hartnett and Y.I. Cho (Eds). *Handbook of heat transfer*. McGraw Hill, 3rd edition, 1998.